PREPRINT · NOT PEER REVIEWED

KENO-VI and Serpent 2 on 71 criticality models with ENDF/B-VIII.0: agreement, a pitfall of Serpent's sector symmetry, and inconsistent probability tables in SCALE's library

The same geometries, nuclides and temperatures in both codes, and what the outliers turned out to be

Claude and Ian Hill

Claude is an AI model developed by Anthropic, which has not reviewed or endorsed this article. Ian Hill directed the work.

Posted 16 November 2026 · Calculations run 11–16 November 2026

ABSTRACT

CE KENO-VI of SCALE 6.3.3, with SCALE's own ENDF/B-VIII.0 continuous-energy library, and Serpent 2.2.1, with the same evaluations processed by NJOY2016, were run on 71 criticality models: 64 MCNP models of IRPhE evaluations and 7 reference spheres. Each model reached the two codes by a separate conversion route, and the two geometries were compared at 6.1 million points without a disagreement. Both codes used the nuclides, atom densities and temperatures of KENO-VI's own mixing tables. For the 65 models where both codes gave k, k(KENO-VI) − k(Serpent) has a weighted mean of +22 ± 5 pcm and χ^2 = 166 for 65 models. The largest differences are +208 ± 42 pcm (UKS1M-SPACE-EXP-001) and −170 ± 48 pcm (TRIGA-FUND-RESR-001). Two outliers led to findings that matter beyond this comparison. First, Serpent's sector symmetry option (`set usym`) reflects neutrons only in delta tracking. In surface tracking, which Serpent uses by default in void and gas, neutrons that reach a symmetry plane leak. This made Serpent's k of a VVER sector model 1290 pcm low; delta tracking throughout (`set dt 1.0`) removes the error, and OpenMC with true reflecting planes confirms the corrected value. Second, in SCALE 6.3.3's ENDF/B-VIII.0 library the probability tables of Mo-95 give elastic cross sections 3–12 % above the same file's point data. Making them consistent lowers KENO-VI's k for a fast system with thick molybdenum by 96 pcm, and over the 16 models with molybdenum rerun so far (of 31 that contain Mo-95), χ^2 falls from 64 to 19. A scan of all 732 probability tables of that library found 29 tables in 19 nuclides whose band averages differ from the point data by more than 1 % (median over the table's energies). The two systems with hydrogen in zirconium hydride are lower in KENO-VI by 131 ± 27 pcm, which is

not explained. The comparison is between codes and processing routes on the same evaluations; no benchmark values are used.

Keywords: KENO-VI; Serpent; SCALE 6.3.3; code-to-code comparison; ENDF/B-VIII.0; criticality; IRPhE; probability tables; unresolved resonance range; thermal scattering; OpenMC

---

1. Introduction

Comparing two Monte Carlo codes on the same models separates the effects of geometry, materials, nuclear-data processing and transport, which a comparison with measurements mixes together. The comparison here has a second purpose. The KENO-VI models were made by csg2csg-keno [1], a converter from MCNP to KENO-VI written in this project, and running the converted models against an independent conversion to another code tests the converter on whole reactors rather than on pictures and points.

KENO-VI [2] was run with SCALE 6.3.3's ENDF/B-VIII.0 continuous-energy library, processed by ORNL with AMPX [3]. Serpent 2 [4] was run with the same ENDF/B-VIII.0 evaluations [5], processed for this work with NJOY2016 [6]. The two codes therefore differ in transport and in processing, but not in the evaluations, the geometry or the material compositions. Where they disagreed by much more than their statistics, a third code, OpenMC [7], and targeted tests were used to find which side was wrong. Section 2 describes the models, data and runs, Section 3 the results and the findings, and Section 4 their limits.

2. Models and methods

2.1 Models and their two conversions

The 64 models are MCNP inputs of evaluations in the IRPhE Handbook [8], identified here by their evaluation identifiers only; the models themselves are not published. They cover fast metal and zero-power assemblies (ZPR, ZPPR, BFS, FCA, SNEAK), research reactors, light-water, heavy-water, graphite and RBMK lattices, and space-reactor mock-ups. The 7 reference problems (REF-…) are single spheres defined for this work: HEU metal, Pu metal, LEU with water, and HEU with heavy water, graphite, polyethylene or zirconium hydride.

Each MCNP model was converted twice, by routes that share no code. KENO-VI inputs were written by csg2csg-keno 0.0.27+keno.1 [1]. Serpent geometries were written by csg2csg's own MCNP reader and Serpent writer [9] followed by a post-processor of this project that handles lattices, transformations and universes the writer leaves out. The two geometries were compared point by point: at each pixel of KENO-VI's own geometry plots, and on further zoomed planes, Serpent was asked which material it finds (`-matpos`). Over the 64 models, 6,135,760 points were compared, with no disagreement apart from four points lying exactly on a surface. Materials that exist in the MCNP model but have no KENO-VI mixture, such as cells that KENO-VI's geometry makes unreachable, were given a flux detector in Serpent; every such detector scored zero.

2.2 Materials

KENO-VI was first run on every model with `run=no`, which writes its mixing table: the nuclides after SCALE's expansion of natural elements, their atom densities, and the temperature of the library data used for each. Serpent's materials were written from these tables, so that both codes transport the same nuclides at the same densities. Bound nuclides (SCALE's thermal-scattering identifiers) were given the neutron table of their fast evaluation and the S(α,β) table of the same thermal evaluation; where KENO-VI interpolates between two kernel temperatures, Serpent interpolates between the same two (`moder` with two tables).

2.3 Nuclear data

KENO-VI read SCALE 6.3.3's `ce_v8.0_endf` library. For Serpent, every nuclide and temperature that KENO-VI used was processed from the ENDF/B-VIII.0 files with NJOY2016.78 (RECONR and BROADR at 0.1 %, GASPR, PURR, ACER; THERMR and ACER for the thermal evaluations of the ENDF/B-VIII.0 thermal sublibrary). Probability tables were on in both codes, and Serpent's on-the-fly broadening was off, since every table is at the temperature KENO-VI uses.

The NJOY tables were checked against LANL's ENDF/B-VIII.0 ACE library Lib80x [10] at 293.6 K for the 261 nuclides of the comparison. Thermal-energy cross sections agree within 1×10^{-5} for 793 of 794 reactions, $\bar{\nu}$ is identical, and the probability tables agree within 4×10^{-5}. Below 1 MeV, all cross sections agree within 1.1 % and most within 10^{-4}; the larger values are single points in deep minima. Above 1 MeV, 14 tables differ because LANL's tables are not Doppler-broadened there (they equal LANL's 0.1 K tables above 1 MeV), while NJOY2016's default broadens to the top of the resolved range. Rerunning four Serpent models with LANL's tables changed k by +63 ± 44, −11 ± 37, −3 ± 39 and −8 ± 38 pcm.

2.4 Runs and statistics

KENO-VI ran 10,000 neutrons per generation, skipped 50 generations and stopped at a standard deviation of 30 pcm or after 12 hours; the k used is the average over the active generations with 50 skipped. Serpent ran 10,000 neutrons per cycle with 100 inactive cycles, and a number of active cycles chosen from a short pilot run to aim at about 20 pcm, with at most 8 hours. Its k is the implicit estimator, except in the 12 models run in optimisation mode 1 to fit in memory, which has no implicit estimator; there the collision estimator is used (marked * in the appendix). The difference d = k(KENO-VI) − k(Serpent) is given in pcm (10^{-5}) with $\sigma = (\sigma_K^2 + \sigma_S^2)^{1/2}$, and $z = d/\sigma$. Means over several models are inverse-variance weighted.

3. Results

3.1 Overview

Both codes gave k for 65 of the 71 models. KENO-VI was too slow for four large lattice models: PROTEUS-GCR-EXP-001 and RBMKCF reached the time limit without a final k, and ATR and IGR were stopped after more than two hours had not completed a generation. In CREOLE, KENO-VI stopped in the first generation with the message that a neutron was outside an array without crossing its boundary, which KENO-VI attributes to a hole overlapping the array boundary: a construct of the converted model that KENO-VI does not accept, and a limitation of the converter for this model. Serpent needed more memory than the machine

had for NRAD. Over the 65 models, the weighted mean of d is +22 ± 5 pcm (unweighted +23 pcm) and χ^2 is 165.9 for 65 values. With exact codes and data, |z| would exceed 2 in about 3 models and 3 in about 0.2; it does in 13 and 4. So the codes agree on average to about 20 pcm, but the scatter is larger than the statistics allow: there are real differences of up to a few hundred pcm in some models. Figure 1 shows d against the energy of average lethargy of fission (EALF), Figure 2 the distribution of z, and Table 1 the models with |z| above 2.5. Every model's values are in the appendix and in keno_serpent_results.csv.

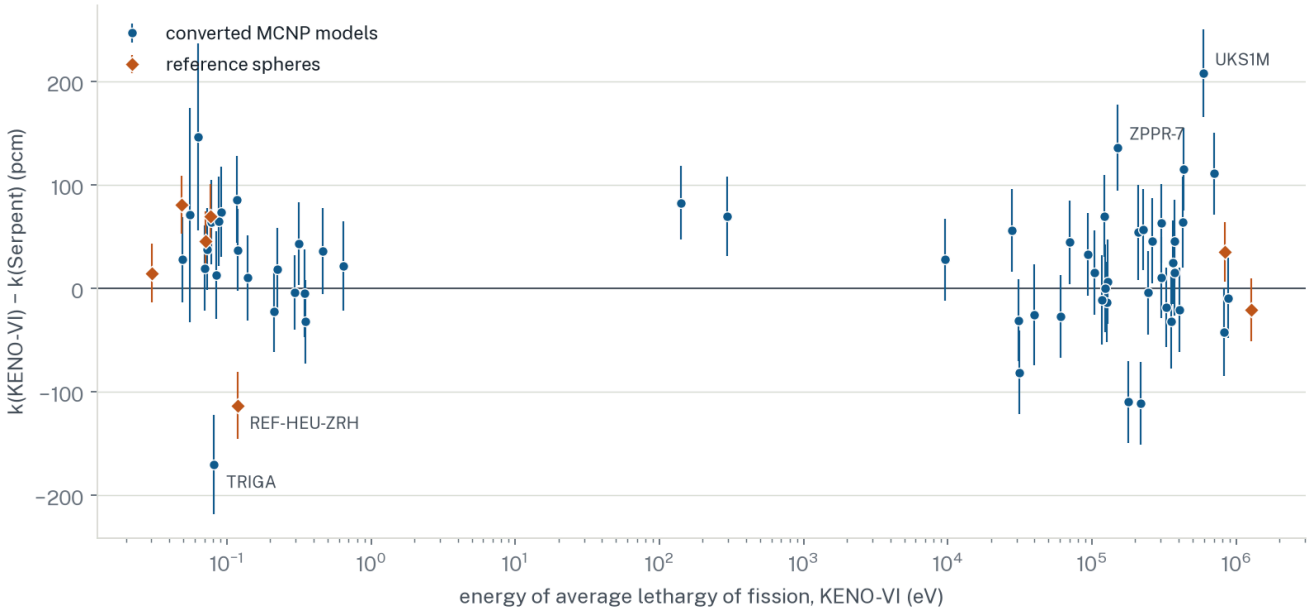

Figure 1. k(KENO-VI) − k(Serpent) against KENO-VI's energy of average lethargy of fission, for the 65 models with both results; bars ±1σ. Models with |z| ≥ 3 are labelled. Serpent values for the two sector models are with `set dt 1.0` (Section 3.2).

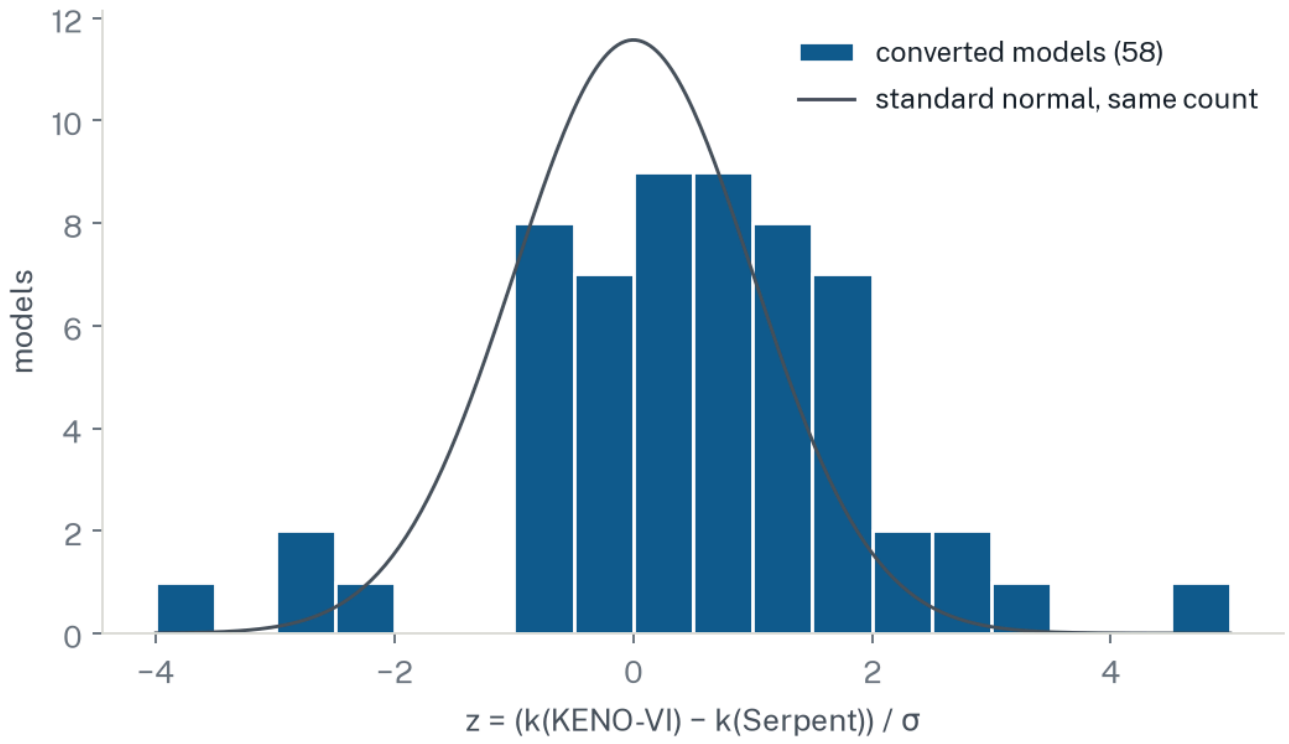

Figure 2. Distribution of z = d/σ for the converted MCNP models, against a standard normal distribution of the same count.

Table 1. Models with |z| above 2.5, with the S(α,β) data they use (Section 3.6).

Model	S(α,β) data	d (pcm)	z
UKS1M-SPACE-EXP-001	none (no S(α,β) data)	+208 ± 42	+4.9
TRIGA-FUND-RESR-001	H in ZrH	−170 ± 48	−3.5
REF-HEU-ZRH	H in ZrH	−113 ± 33	−3.5
ZPPR-LMFR-EXP-007	none (no S(α,β) data)	+136 ± 42	+3.3
REF-HEU-POLY	H in polyethylene	+81 ± 28	+2.9
ZPR-FUND-EXP-001	none (no S(α,β) data)	+116 ± 40	+2.9
CORALI-FUND-RESR-001	none (no S(α,β) data)	+111 ± 40	+2.8
SNEAK-LMFR-EXP-001	graphite (no D_2O)	−111 ± 40	−2.8
ZPR-FUND-EXP-014	none (no S(α,β) data)	−110 ± 39	−2.8

3.2 Serpent's sector symmetry leaks in surface tracking

Two models are reactor sectors bounded by reflecting planes: a 60° sector of LR-VVER-RESR-001 and a quarter of PBF-FUND-RESR-001. In Serpent they were run as full geometries with the sector symmetry option `set usym`, which folds the full model into the sector by reflection; Serpent's planes must pass through the origin. With Serpent's defaults, LR-VVER gave 0.98755 ± 27 against KENO-VI's 1.00045 ± 30, a

difference of +1290 ± 40 pcm. The geometry agreed point by point, also within 0.05 cm of the planes; the materials, the LANL tables and the symmetry mode made no difference; and with vacuum instead of reflecting planes the codes agreed (KENO-VI 0.58639 ± 86, Serpent 0.58665 ± 34).

OpenMC was then used as a third code. A converter of this project wrote the Serpent model, with KENO-VI's materials, as an OpenMC model with true reflecting planes, and the material found at 50,000 points agreed with Serpent's everywhere. OpenMC gave 1.00025 ± 14, +20 ± 33 pcm from KENO-VI (vacuum planes: 0.58603 ± 12), and its leakage fraction was 0.0374 against Serpent's 0.0501: 1.27 percentage points, the size of Serpent's deficit. So Serpent was losing neutrons at the planes.

Small tests located the cause (Table 2): a cylinder of fuel with a void gap and water around it, cut to a 60° sector. With the planes and default tracking, k was 998 pcm below the full model. It agreed with the full model when Serpent was forced to use delta tracking everywhere (`set dt 1.0`) and fell by 13,700 pcm with surface tracking everywhere (`set dt 0.0`). Serpent switches from delta to surface tracking where a material's total cross section is below a fraction of the majorant, by default in void and gas. The reflection of `usym` is applied in delta tracking only; a neutron that reaches a plane in surface tracking enters the cells beyond it and leaks. LR-VVER has void above the water and inside its pins. The earlier tests of `usym` in this project had no void and so never left delta tracking. With `set dt 1.0`, LR-VVER gives 1.00026 ± 26, +19 ± 40 pcm from KENO-VI, and PBF −4 ± 36 pcm; both are the values used in this paper.

Table 2. Serpent 2.2.1 on a small test of `set usym`: fuel cylinder (radius 20 cm, height 40 cm), void gap from 20 to 22 cm, water from 22 to 30 cm, void above; 60° sector between 60° and 120°.

Case	k	Leakage
Full model	0.92793 ± 48	0.149
Sector, reflecting planes in the geometry, default tracking	0.91795 ± 50	0.164
Sector, planes removed (usym only)	0.92855 ± 46	
Sector with planes, `set dt 1.0` (delta tracking only)	0.92843 ± 50	
Sector with planes, `set dt 0.0` (surface tracking only)	0.79080 ± 47	0.287
Full model, `set dt 0.0`	0.92890 ± 41	

Standard deviations in pcm; leakage fractions where recorded. Without the planes in the geometry, a neutron that crosses the sector boundary in surface tracking continues in the rest of the full model, which by symmetry gives the same k; LR-VVER without its planes gave 1.00048 ± 44.

3.3 UKS1M: inconsistent Mo-95 probability tables in SCALE's library

UKS1M-SPACE-EXP-001, a fast highly enriched uranium system with thick molybdenum and about 48 % leakage, has the largest difference: KENO-VI 0.99719 ± 30, Serpent 0.99511 ± 30, d = +208 ± 42 pcm (z = 4.9). The LANL tables moved Serpent by only +63 ± 44 pcm (Section 2.3). OpenMC, with the same model converter and Serpent's data, gave 0.99577 ± 11: KENO-VI − OpenMC = +142 ± 32 pcm and OpenMC − Serpent = +66 ± 32 pcm. So most of the difference was on the KENO-VI side.

The probability tables of the unresolved resonance range were the first suspect: turning them off lowered OpenMC's k by −127 ± 16 pcm (`ptables = False`: 0.99704 ± 11) but KENO-VI's by only −54 ± 42 pcm (`ptb=no`: 0.99773 ± 29). A comparison of SCALE's point cross sections of the UKS1M nuclides with the NJOY tables found the fast integrals within 0.12 %, apart from capture of Mo-95, U-234 and Mo-100 (up to 1.1 %, in the unresolved range). The probability tables themselves were the cause. In SCALE's file, the band-averaged elastic cross section of Mo-95 is 3–12 % above the same file's point elastic cross section over the whole unresolved range, 2.1–206 keV. The band averages should reproduce the point data, and in the NJOY tables, and in this project's AMPX processing of ENDF/B-VIII.1 [11], whose Mo-95 has the same resonance data, they do. Mo-95's capture tables, the other molybdenum isotopes and U-235 and U-238 are consistent.

To test the effect, a copy of SCALE's library was made in which Mo-95's elastic band values are scaled, row by row, to the point elastic cross section, and its total band values shifted by the same amounts. With it, KENO-VI gives 0.99623 ± 30 for UKS1M, a change of −96 ± 42 pcm, and KENO-VI − OpenMC falls from +142 ± 32 to +46 ± 32 pcm. KENO-VI − Serpent is then +112 ± 42 pcm, which leaves OpenMC − Serpent, +66 ± 32 pcm, as the largest remaining part; it was not investigated further.

3.4 The other models with molybdenum

Mo-95 is in 31 of the models, often only through the molybdenum of stainless steel. So far 17 of them have been rerun with the corrected Mo-95 tables (Table 3, Figure 3); the other 12 with a KENO-VI result (SNEAK-LMFR-EXP-001, TRIGA-FUND-RESR-001, ZPR-FUND-EXP-008, ZPR-FUND-EXP-009, ZPR-FUND-EXP-010, ZPR-FUND-EXP-011, ZPR-FUND-EXP-012, ZPR-FUND-EXP-013, ZPR-FUND-EXP-015, ZPR-FUND-EXP-016, ZPR-LMFR-EXP-001, ZPR-LMFR-EXP-002) have not, and Table 3 is not a complete account. The largest changes are in fast systems: ZPPR-LMFR-EXP-007 changes by −115 pcm and ZPR-FUND-EXP-001 by −75 pcm, and their differences from Serpent fall from +136 and +116 to +21 and +40 pcm. Over the 16 models with both codes, χ^2 falls from 63.6 to 18.6 (for 16 values). The three KRITZ lattices, thermal systems with little molybdenum, move by −39 ± 24 pcm on average, which makes their agreement with Serpent slightly worse; this may be statistical (1.6σ). Over all 65 models, replacing the KENO-VI values of these 16 by the corrected ones changes χ^2 from 165.9 to 121.0 and the weighted mean of d to +16 ± 5 pcm. The corrected library is a local test only; everything else in this paper uses SCALE's library as shipped.

Table 3. KENO-VI with Mo-95's probability tables made consistent with its point data: change of k, and k(KENO-VI) − k(Serpent) before and after (pcm).

Model	Change of KENO-VI k	d, library as shipped	d, Mo-95 consistent
FCA-FUND-EXP-001	−26 ± 42	+64 ± 44	+38 ± 44
FFTF-LMFR-RESR-001	−43 ± 42	+15 ± 41	−28 ± 41
KRITZ-LWR-RESR-001	−39 ± 42	+10 ± 41	−29 ± 41
KRITZ-LWR-RESR-002	−37 ± 42	−32 ± 40	−69 ± 40
KRITZ-LWR-RESR-003	−42 ± 42	−22 ± 39	−64 ± 39
NRAD-FUND-RESR-001	−4 ± 42	–	–
SCCA-SPACE-EXP-002	+59 ± 42	−81 ± 40	−22 ± 40
UKS1M-SPACE-EXP-001	−96 ± 42	+208 ± 42	+112 ± 42
ZPPR-LMFR-EXP-001	−10 ± 44	−11 ± 43	−21 ± 42
ZPPR-LMFR-EXP-007	−115 ± 42	+136 ± 42	+21 ± 42
ZPPR-LMFR-EXP-010	−27 ± 45	+54 ± 46	+27 ± 43
ZPR-FUND-EXP-001	−75 ± 41	+116 ± 40	+40 ± 42
ZPR-FUND-EXP-002	+0 ± 42	−21 ± 41	−21 ± 41
ZPR-FUND-EXP-003	−2 ± 42	+46 ± 41	+44 ± 41
ZPR-FUND-EXP-006	+7 ± 42	−27 ± 40	−20 ± 40
ZPR-FUND-EXP-007	−37 ± 42	+56 ± 40	+19 ± 40
ZPR-FUND-EXP-014	+90 ± 42	−110 ± 39	−20 ± 39

NRAD has no Serpent result (Section 3.1).

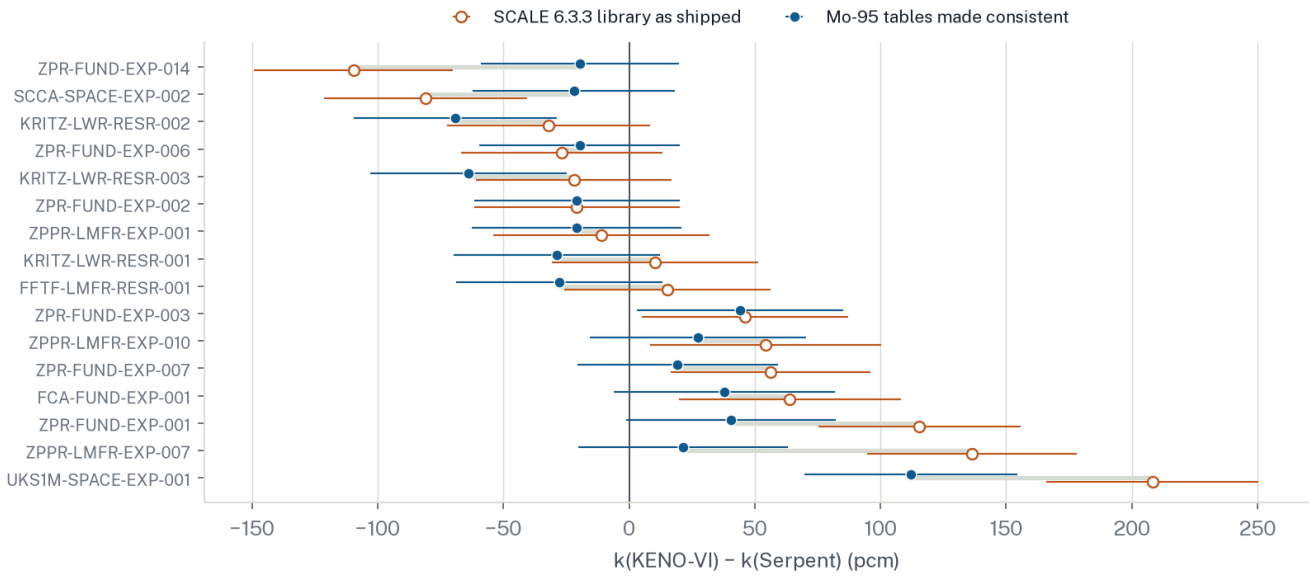

Figure 3. k(KENO-VI) − k(Serpent) for the models with molybdenum, with SCALE 6.3.3's library as shipped (open) and with Mo-95's probability tables made consistent with its point data (filled); bars ±1σ.

3.5 Probability tables of the whole SCALE library

Every probability table of SCALE 6.3.3's `ce_v8.0_endf` at 293 K (732 tables of elastic, fission and capture) was compared with the same file's point cross section at each table energy. Table 4 lists the 29 tables in 19 nuclides whose band average differs from the point value by more than 1 %, as the median over the table's energies. Several are nuclides of little weight in criticality, but U-236, U-240, U-241 and Pu-243 occur in irradiated fuel, and U-236 is in 29 of the models of this comparison; its tables differ by 5–6 % in fission and capture, and its effect on k was not tested. Many more tables differ at their first energies only; a lower-edge problem of this kind was found and corrected in the ENDF/B-VIII.1 library of this project [11].

Table 4. Probability tables of SCALE 6.3.3's ENDF/B-VIII.0 library at 293 K whose band-averaged cross section differs from the same file's point cross section by more than 1 % (median of |band average/point − 1| over the table energies), with the largest signed difference.

Nuclide	Reaction	Median |Δ| (%)	Largest Δ (%)	Table range
Ar-38	capture	72.5	−84	300 keV–1.2 MeV
U-241	fission	28.9	−97	102 eV–10 keV
Ar-38	elastic	28.5	−40	300 keV–1.2 MeV
Pu-243	capture	22.2	+91	102 eV–10 keV
Ar-36	elastic	21.5	−42	46.5 keV–1.2 MeV
U-240	capture	21.3	+89	986 eV–10 keV
U-241	capture	20.8	+92	102 eV–10 keV
Ar-36	capture	18.3	−84	46.5 keV–1.2 MeV
Nd-144	elastic	17.9	+20	9.97 keV–250 keV
Pu-243	fission	12.4	+90	102 eV–10 keV
Pd-105	elastic	12.4	+25	2.05 keV–283 keV
Mo-95	elastic	10.2	+13	2.14 keV–206 keV
U-240	fission	10.0	−27	986 eV–10 keV
Ge-70	capture	7.8	−31	14 keV–1.05 MeV
U-240	elastic	7.7	+24	986 eV–10 keV
U-236	capture	6.4	−8	1.5 keV–100 keV
U-236	fission	5.2	−6	1.5 keV–100 keV
U-241	elastic	4.2	+24	102 eV–10 keV
Ru-101	elastic	3.3	+14	1.03 keV–128 keV
Pu-243	elastic	3.0	+7	102 eV–10 keV
Dy-160	elastic	2.8	+15	2.01 keV–87.3 keV
Dy-160	capture	2.6	+85	2.01 keV–87.3 keV
Ge-74	capture	2.1	−36	6 keV–604 keV
Cd-111	capture	1.6	+30	2.3 keV–100 keV
Cd-106	capture	1.4	+30	6 keV–100 keV
Er-167	elastic	1.3	−1	1.75 keV–10 keV

Nuclide	Reaction	Median |Δ| (%)	Largest Δ (%)	Table range
Sr-89	elastic	1.2	+27	1.4 keV–100 keV
Xe-131	elastic	1.1	−5	3.94 keV–80.8 keV
Eu-154	capture	1.1	+6	27.5 eV–100 keV

Equiprobable bands; the band average is the mean of the band values. The scan does not say which of the two, the table or the point data, departs from the evaluation, but for Mo-95 the point data agree with NJOY (Section 3.3).

3.6 Differences by thermal-scattering data and spectrum

Table 5 groups the models by the S(α,β) data they use. The 8 light-water systems without other kernels agree well, +17 ± 13 pcm with $\chi^2 = 6.9$. The two systems with hydrogen in zirconium hydride, TRIGA-FUND-RESR-001 (−170 ± 48 pcm) and the reference sphere REF-HEU-ZRH (−113 ± 33 pcm), are both low in KENO-VI, by 131 ± 27 pcm on average; since the reference sphere has nothing but HEU and ZrH, the zirconium hydride data or their use are the likely place to look, but the cause was not investigated. The graphite systems scatter on both sides of zero, and the D_2O systems lean positive (+31 ± 12 pcm). By spectrum (Table 6), fast and thermal systems have similar means.

Table 5. k(KENO-VI) − k(Serpent) by the S(α,β) data in the model (each model in the first group that applies).

S(α,β) data	Models	Weighted mean d (pcm)	χ^2	Models
H in ZrH	2	−131 ± 27	24.5	TRIGA-FUND-RESR-001, REF-HEU-ZRH
H in polyethylene	2	+57 ± 23	8.4	BFS1-FUND-EXP-002, REF-HEU-POLY
D in D_2O (with or without others)	12	+31 ± 12	11.7	ETA-HWR-EXP-001, ETA-HWR-EXP-002, PROTEUS-GCR-EXP-003, PROTEUS-GCR-EXP-004, RB-FUND-EXP-001, RB-FUND-EXP-002, RB-FUND-EXP-003, RB-FUND-EXP-004, RB-FUND-EXP-005, SSCR-PWR-EXP-002, ZED2-HWR-EXP-001, REF-HEU-D2O
graphite (no D_2O)	8	+24 ± 13	31.2	HECTOR-FUND-EXP-001, HECTOR-FUND-EXP-002, HTTR-GCR-RESR-001, HTTR-GCR-RESR-003, SCCA-SPACE-EXP-001, SCCA-SPACE-EXP-002, SNEAK-LMFR-EXP-001, REF-HEU-GRAPHITE
H in H_2O only	8	+17 ± 13	6.9	KRITZ-LWR-RESR-001, KRITZ-LWR-RESR-002, KRITZ-LWR-RESR-003, LR-VVER-RESR-001, PBF-FUND-RESR-001, RA6-FUND-RESR-001, SSCR-PWR-EXP-001, REF-LEU-H2O
beryllium only	1	−25 ± 49	0.3	SCCA-SPACE-EXP-003
none (no S(α,β) data)	32	+27 ± 7	83.0	32 cases, mostly fast systems

Table 6. k(KENO-VI) − k(Serpent) by KENO-VI's energy of average lethargy of fission.

Spectrum	Models	Weighted mean d (pcm)	χ^2
EALF below 1 eV	26	+22 ± 8	61.9
EALF 1 eV to 10 keV	3	+62 ± 22	9.2
EALF above 10 keV	36	+18 ± 7	94.8

4. Discussion

What the comparison shows. Two conversions that share no code give the same geometry at 6.1 million points, and with the same materials the two codes agree on average within about 20 pcm. For most models KENO-VI and Serpent agree within their statistics, which supports both the converted KENO-VI models and the Serpent models. The differences that remain beyond the statistics were, where they were followed up, problems in one code's input options or in one processed library, not in the conversion: Serpent's sector symmetry in surface tracking, and SCALE's Mo-95 probability tables.

The Serpent finding. The `usym` leak is silent: Serpent gives no warning, and the result looks reasonable. It affects any sector model with void or gas reaching the symmetry planes, which is common in reactor models (gaps, plenums, voided channels). Delta tracking throughout is a simple remedy; whether Serpent intends `usym` to be used only with delta tracking is not stated in its input manual [12] as far as we found.

The SCALE finding. Probability tables whose band averages do not reproduce the point data change the cross sections in the unresolved range. For UKS1M the effect is about 100 pcm. In most of the 29 tables of Table 4 the effect on criticality calculations is probably small, because the nuclides are rare or their unresolved range matters little. U-236, present in many fuels, is an exception worth a test. The scan compares each table with its own file only; whether the defects come from the processing or from how the evaluation's unresolved parameters were used was not examined.

Limits. This is a comparison between codes and between processing routes, with the same evaluations. It does not test the evaluations, and agreement does not mean that either code is right. Differences in how the codes treat thermal scattering, probability tables and secondary distributions are included in d and cannot be separated from processing differences without further tests. Of the remaining outliers, TRIGA and REF-HEU-ZRH (zirconium hydride), the remaining UKS1M difference between OpenMC and Serpent, and SNEAK-LMFR-EXP-001 were not investigated. Four models were too slow in KENO-VI, and one converted model (CREOLE) is not accepted by KENO-VI's tracking. The handbook's benchmark values were not used.

5. Conclusions

- On 65 criticality models, KENO-VI (SCALE 6.3.3, SCALE's ENDF/B-VIII.0 library) and Serpent 2.2.1 (NJOY2016 ENDF/B-VIII.0) agree on average, +22 ± 5 pcm, with $\chi^2 = 165.9$; the geometry of the two independent conversions agrees at 6.1 million points.
- Serpent's `set usym` reflects neutrons only in delta tracking. Neutrons in surface tracking (void and gas by default) leak through the symmetry planes. A VVER sector model was 1290 pcm low; `set dt 1.0` corrects it, as OpenMC with true reflecting planes confirms.
- SCALE 6.3.3's ENDF/B-VIII.0 library has Mo-95 probability tables whose elastic band averages are 3–12 % above its point data; correcting them moves KENO-VI by up to −115 pcm in the molybdenum-bearing models rerun so far and reduces their χ^2 from 64 to 19 (16 models). 29 tables in 19 nuclides of the library are more than 1 % inconsistent in the same way.
- Open: KENO-VI is 131 ± 27 pcm below Serpent in the two systems with zirconium hydride, and OpenMC is 66 ± 32 pcm above Serpent in UKS1M.

About the authors and the status of this work

> Claude is an AI model developed by Anthropic. Ian Hill proposed the comparison, chose the data (ENDF/B-VIII.0 processed with NJOY for Serpent, against SCALE's own library for KENO-VI), provided the MCNP models and the codes, asked for the OpenMC check of the VVER sector, the comparison with LANL's tables and the investigation of UKS1M, and directed the work. Claude wrote csg2csg-keno, the post-processor of the Serpent route, the OpenMC converter and the comparison scripts, processed the data, ran the calculations, investigated the outliers, made the figures and tables, and wrote this article. The article has not been peer reviewed, and the results have not been independently reviewed or verified. Anthropic has not reviewed or endorsed this work.

Data and code availability

The results of every model are in keno_serpent_results.csv (CC BY 4.0): KENO-VI and Serpent k with standard deviations, the Serpent estimator, d, σ, z, EALF, the S(α,β) group, and the KENO-VI k with consistent Mo-95 tables where it was run. The KENO-VI converter is published [1]. The converted models, the comparison scripts that read them, the modified SCALE library of Section 3.3 and the scan of Section 3.5 stay local: the models derive from the IRPhE Handbook, and SCALE's data are distributed under licence. No values from the handbook (benchmark k or the handbook's own calculations) are used or published.

References

[1] Claude and Ian Hill, *csg2csg-keno: MCNP to SCALE KENO-VI converter*, version 0.0.27+keno.1 (2026), https://doi.org/10.5281/zenodo.24137058; https://hardtohit10.gitlab.io/csg2csg-keno.html.

[2] W.A. Wieselquist, R.A. Lefebvre (Eds.), *SCALE 6.3.1 User Manual*, ORNL/TM-SCALE-6.3.1, Oak Ridge National Laboratory (2023): the KENO chapter.

[3] D. Wiarda, M.E. Dunn, N.M. Greene, M.L. Williams, C. Celik, L.M. Petrie, *AMPX-6: A Modular Code System for Processing ENDF/B*, ORNL/TM-2016/43, Oak Ridge National Laboratory (2016).

[4] J. Leppänen, M. Pusa, T. Viitanen, V. Valtavirta, T. Kaltiaisenaho, “The Serpent Monte Carlo code: Status, development and applications in 2013”, *Annals of Nuclear Energy* 82 (2015) 142–150.

[5] D.A. Brown et al., “ENDF/B-VIII.0: The 8th Major Release of the Nuclear Reaction Data Library with CIELO-project Cross Sections, New Standards and Thermal Scattering Data”, *Nuclear Data Sheets* 148 (2018) 1–142.

[6] D.W. Muir, R.M. Boicourt, A.C. Kahler, J.L. Conlin, W. Haeck, *The NJOY Nuclear Data Processing System, Version 2016*, LA-UR-17-20093, Los Alamos National Laboratory (2016).

[7] P.K. Romano, N.E. Horelik, B.R. Herman, A.G. Nelson, B. Forget, K. Smith, "OpenMC: A state-of-the-art Monte Carlo code for research and development", *Annals of Nuclear Energy* 82 (2015) 90–97.

[8] *International Handbook of Evaluated Reactor Physics Benchmark Experiments*, NEA/NSC/DOC(2006)1, OECD Nuclear Energy Agency.

[9] A. Davis, *csg2csg*, a converter between Monte Carlo constructive solid geometry formats, https://github.com/makeclean/csg2csg.

[10] Los Alamos National Laboratory, Nuclear Data Team, *Lib80x: ENDF/B-VIII.0 based ACE library*, and the ENDF80SaB2 thermal library, https://nucleardata.lanl.gov/ace/lib80x/ (downloaded 12 November 2026).

[11] Claude and Ian Hill, "An ENDF/B-VIII.1 continuous-energy neutron library for SCALE, processed with AMPX", preprint, https://hardtohit10.gitlab.io/ampx-ce-paper.html (2026).

[12] Serpent Wiki, *Input syntax manual*: `set usym` and `set dt`, https://serpent.vtt.fi/mediawiki/index.php/Input_syntax_manual.

Appendix: every model

k of all 71 models in both codes

Model	KENO-VI k ± pcm	Serpent k ± pcm	d (pcm)	z	EALF (eV)
ATR-FUND-RESR-001	KENO-VI: too slow (no generation completed in over 2 h), stopped				
BFS1-FUND-EXP-001	0.98964 ± 30	0.98996 ± 35	−32 ± 46	−0.7	3.55e+05
BFS1-FUND-EXP-002	0.99674 ± 30	0.99663 ± 25	+11 ± 39	+0.3	3.01e+05
BFS1-FUND-EXP-004	0.99635 ± 30	0.99639 ± 27	−4 ± 40	−0.1	2.44e+05
BFS2-FUND-EXP-001	1.00579 ± 30	1.00546 ± 26	+33 ± 40	+0.8	9.44e+04
BR2-LMFR-RESR-001	1.00211 ± 30	1.00220 ± 25	−9 ± 39	−0.2	8.84e+05
CORALI-FUND-RESR-001	1.00118 ± 30	1.00007 ± 26	+111 ± 40	+2.8	7.06e+05
CREOLE-PWR-EXP-001	KENO-VI: stopped in generation 1 (k6-262, hole overlapping an array boundary in the converted model)				
ETA-HWR-EXP-001	0.99457 ± 30	0.99462 ± 30	−5 ± 42	−0.1	0.346

Model	KENO-VI k ± pcm	Serpent k ± pcm	d (pcm)	z	EALF (eV)
ETA-HWR-EXP-002	0.99742 ± 30	0.99699 ± 27	+43 ± 40	+1.1	0.317
FCA-FUND-EXP-001	1.00920 ± 30	1.00856 ± 32	+64 ± 44	+1.5	4.25e+05
FFTF-LMFR-RESR-001	0.99672 ± 30	0.99657 ± 28*	+15 ± 41	+0.4	1.04e+05
HECTOR-FUND-EXP-001	1.00827 ± 30	1.00757 ± 24	+70 ± 39	+1.8	295
HECTOR-FUND-EXP-002	1.01545 ± 30	1.01462 ± 19	+83 ± 36	+2.3	141
HTTR-GCR-RESR-001	1.01839 ± 30	1.01775 ± 27*	+64 ± 41	+1.6	0.0784
HTTR-GCR-RESR-003	1.01529 ± 30	1.01455 ± 31*	+74 ± 43	+1.7	0.0917
IGR-FUND-RESR-001	KENO-VI: too slow (no generation completed in over 2 h), stopped				
KRITZ-LWR-RESR-001	0.99929 ± 30	0.99919 ± 28	+10 ± 41	+0.3	0.139
KRITZ-LWR-RESR-002	0.99793 ± 30	0.99825 ± 27	−32 ± 40	−0.8	0.349
KRITZ-LWR-RESR-003	1.00047 ± 30	1.00069 ± 25	−22 ± 39	−0.6	0.213
LR-VVER-RESR-001	1.00045 ± 30	1.00026 ± 26	+19 ± 40	+0.5	0.224
NRAD-FUND-RESR-001	Serpent: more memory than available (9.4 GB), also in optimisation mode 1				
ORSPHERE-FUND-EXP-001	1.00381 ± 30	1.00423 ± 30	−42 ± 43	−1.0	8.27e+05
PBF-FUND-RESR-001	1.01795 ± 28	1.01799 ± 22	−4 ± 36	−0.1	0.297
PROTEUS-GCR-EXP-001	KENO-VI: no final k within the time limit				
PROTEUS-GCR-EXP-003	0.99742 ± 84	0.99595 ± 34*	+147 ± 91	+1.6	0.0631
PROTEUS-GCR-EXP-004	0.99496 ± 100	0.99425 ± 27*	+71 ± 104	+0.7	0.0553
RA6-FUND-RESR-001	1.00104 ± 30	1.00039 ± 31	+65 ± 43	+1.5	0.0881
RB-FUND-EXP-001	0.99962 ± 30	0.99924 ± 26	+38 ± 40	+1.0	0.0733
RB-FUND-EXP-002	0.99921 ± 30	0.99901 ± 28	+20 ± 41	+0.5	0.0707

Model	KENO-VI k ± pcm	Serpent k ± pcm	d (pcm)	z	EALF (eV)
RB-FUND-EXP-003	0.99739 ± 30	0.99702 ± 26	+37 ± 40	+0.9	0.119
RB-FUND-EXP-004	1.00661 ± 30	1.00633 ± 28	+28 ± 41	+0.7	0.0493
RB-FUND-EXP-005	1.00101 ± 30	1.00088 ± 30	+13 ± 42	+0.3	0.0841
RBMKCF-RBMK-EXP-001	KENO-VI: no final k within the time limit				
SCCA-SPACE-EXP-001	1.00117 ± 30	1.00130 ± 24	−13 ± 38	−0.3	1.28e+05
SCCA-SPACE-EXP-002	0.99998 ± 30	1.00079 ± 27*	−81 ± 40	−2.0	3.14e+04
SCCA-SPACE-EXP-003	0.99589 ± 41	0.99614 ± 27*	−25 ± 49	−0.5	3.96e+04
SNEAK-LMFR-EXP-001	1.00247 ± 30	1.00358 ± 26	−111 ± 40	−2.8	2.17e+05
SSCR-PWR-EXP-001	0.99921 ± 30	0.99884 ± 29	+37 ± 42	+0.9	0.465
SSCR-PWR-EXP-002	1.01122 ± 30	1.01100 ± 31	+22 ± 43	+0.5	0.639
TRIGA-FUND-RESR-001	1.00376 ± 38	1.00546 ± 29	−170 ± 48	−3.5	0.0817
UKS1M-SPACE-EXP-001	0.99719 ± 30	0.99511 ± 30	+208 ± 42	+4.9	5.9e+05
ZED2-HWR-EXP-001	0.99861 ± 31	0.99775 ± 28	+86 ± 42	+2.1	0.117
ZPPR-LMFR-EXP-001	0.99835 ± 32	0.99846 ± 29*	−11 ± 43	−0.3	1.17e+05
ZPPR-LMFR-EXP-007	0.99924 ± 30	0.99788 ± 29*	+136 ± 42	+3.3	1.51e+05
ZPPR-LMFR-EXP-010	0.99815 ± 34	0.99761 ± 31*	+54 ± 46	+1.2	2.1e+05
ZPR-FUND-EXP-001	0.99824 ± 28	0.99708 ± 29	+116 ± 40	+2.9	4.32e+05
ZPR-FUND-EXP-002	0.99538 ± 30	0.99559 ± 28	−21 ± 41	−0.5	4.04e+05
ZPR-FUND-EXP-003	0.99829 ± 30	0.99783 ± 28	+46 ± 41	+1.1	2.64e+05
ZPR-FUND-EXP-004	0.99759 ± 30	0.99744 ± 28	+15 ± 41	+0.4	3.72e+05
ZPR-FUND-EXP-005	1.00161 ± 30	1.00179 ± 24	−18 ± 38	−0.5	3.27e+05

Model	KENO-VI k ± pcm	Serpent k ± pcm	d (pcm)	z	EALF (eV)
ZPR-FUND-EXP-006	0.97945 ± 30	0.97972 ± 26	−27 ± 40	−0.7	6.07e+04
ZPR-FUND-EXP-007	0.97076 ± 30	0.97020 ± 26	+56 ± 40	+1.4	2.78e+04
ZPR-FUND-EXP-008	0.99249 ± 30	0.99204 ± 27	+45 ± 40	+1.1	7.03e+04
ZPR-FUND-EXP-009	1.00390 ± 30	1.00362 ± 26	+28 ± 40	+0.7	9.64e+03
ZPR-FUND-EXP-010	0.99657 ± 30	0.99611 ± 27	+46 ± 40	+1.1	3.75e+05
ZPR-FUND-EXP-011	0.99740 ± 30	0.99677 ± 23	+63 ± 38	+1.7	3.04e+05
ZPR-FUND-EXP-012	1.00286 ± 30	1.00229 ± 25	+57 ± 39	+1.5	2.27e+05
ZPR-FUND-EXP-013	1.00278 ± 30	1.00208 ± 26	+70 ± 40	+1.8	1.21e+05
ZPR-FUND-EXP-014	0.98678 ± 30	0.98788 ± 26	−110 ± 39	−2.8	1.79e+05
ZPR-FUND-EXP-015	0.99804 ± 30	0.99835 ± 26	−31 ± 40	−0.8	3.09e+04
ZPR-FUND-EXP-016	0.99554 ± 30	0.99529 ± 27	+25 ± 40	+0.6	3.64e+05
ZPR-LMFR-EXP-001	0.99635 ± 30	0.99628 ± 28*	+7 ± 41	+0.2	1.29e+05
ZPR-LMFR-EXP-002	0.99775 ± 32	0.99775 ± 28*	+0 ± 42	+0.0	1.23e+05
REF-HEU-D2O	1.39793 ± 16	1.39778 ± 24	+15 ± 29	+0.5	0.0303
REF-HEU-GRAPHITE	1.17112 ± 17	1.17042 ± 26	+70 ± 31	+2.3	0.0767
REF-HEU-METAL	0.99656 ± 12	0.99621 ± 26	+35 ± 29	+1.2	8.31e+05
REF-HEU-POLY	1.54387 ± 10	1.54306 ± 26	+81 ± 28	+2.9	0.0485
REF-HEU-ZRH	1.30506 ± 13	1.30619 ± 30	−113 ± 33	−3.5	0.119
REF-LEU-H2O	1.31891 ± 11	1.31845 ± 26	+46 ± 29	+1.6	0.0716
REF-PU-METAL	0.99785 ± 14	0.99806 ± 27	−21 ± 30	−0.7	1.27e+06

* Serpent collision estimator (optimisation mode 1). KENO-VI with SCALE 6.3.3's library as shipped. These are calculated values of converted models, not benchmark values.

By Claude (Anthropic AI model) and Ian Hill · not peer reviewed

Visits are counted with GoatCounter, without cookies or personal data Posted 16 November 2026